Topological states and braiding statistics using quantum circuits

J. Q. You,[1,2] Xiao-Feng Shi,[1,2] and Franco Nori[2,3]

[1]*Department of Physics and Surface Physics Laboratory (National Key Laboratory), Fudan University, Shanghai 200433, China*
[2]*Advanced Study Institute, The Institute of Physical and Chemical Research (RIKEN), Wako-shi 351-0198, Japan*
[3]*Center for Theoretical Physics, Physics Department, Center for the Study of Complex Systems, University of Michigan, Ann Arbor, MI 48109-1040, USA*

(Dated: August 30, 2008)

Using superconducting quantum circuits, we propose an approach to construct a Kitaev lattice, i.e., an anisotropic spin model on a honeycomb lattice with three types of nearest-neighbor interactions. We study two particular cases to demonstrate topological states (i.e., the vortex and bond states) and show how the braiding statistics can be revealed. Our approach provides an experimentally realizable many-body system for demonstrating exotic properties of topological phases.

Topological quantum systems are currently attracting considerable interest because of their fundamental importance and potential applications in quantum computing [1]. They exhibit topological phases of matter that are insensitive to local perturbations. This exotic property makes them appealing for fault-tolerant quantum computing.

Topological quantum computing can be implemented by storing and processing quantum information with anyons [1], which are neither bosons nor fermions, but obey anyonic braiding statistics. To achieve this, it is a centrally important issue to experimentally realize a topological quantum system. Recently, topological quantum computing using non-Abelian anyons in a fractional quantum Hall system was proposed [2]; however, it has not been experimentally verified if the observed fractional quantum Hall states are the desired topological states for quantum computing. Indeed, up to now, anyons have never been directly observed in experiments. Thus, in order to guarantee anyonic topological phases in a many-body quantum system, one could design artificial, but exactly solvable lattice models that have such desired topological phases. The most important example is the Kitaev model on a honeycomb lattice [3], which is an anisotropic spin model with three types of nearest-neighbor interactions. Most strikingly, depending on the bond parameters, this model [3] supports both Abelian and non-Abelian anyons. Therefore, if this topological model could be realized in experiments, it would provide exciting opportunities for experimentally demonstrating anyons and implementing topological quantum computing.

Proposals were made for implementing the Kitaev model using atomic optical lattices [4, 5]. Also, it was shown [6] that optical lattices can be used to demonstrate the anyonic braiding statistics. However, its implementation using an optical lattice requires extremely low temperatures [4] that are beyond current experimental capabilities. Moreover, to demonstrate anyonic braiding, the optical lattice needs to perform rotations on single atoms at selected sites using external laser beams. This is difficult because the atomic spacing is of the order of laser wavelength and the diffraction limit takes effect.

Here we propose an approach to construct a Kitaev lattice using superconducting quantum circuits [7]. A charge qubit is placed at each site and the three types of nearest-neighbor interactions are achieved using different circuit elements. This circuit can demonstrate topological states (i.e., the vortex and bond states) and show how the braiding statistics can be revealed. Here, the quantum circuits behave like artificial spins [7] and the Kitaev model can be constructed using the experimentally available technologies for superconducting qubits. Moreover, these charge qubits are tunable via external fields, making the required single-qubit rotations implementable for demonstrating the braiding statistics of the topological states. Our proposal provides an experimentally realizable many-body system for demonstrating exotic properties of the topological phases.

Kitaev model.—We use superconducting quantum circuits to construct an artificial Kitaev lattice (see Fig. 1). The building block of the lattice consists of four charge qubits [Fig. 1(a)], each placed at a lattice site of a hexagonal lattice [Fig. 1(b)]. Here, each charge qubit is a Cooper-pair box connected to a superconducting ring by two identical Josephson junctions. Each qubit is controlled by both the magnetic flux Φ_i piercing the SQUID loop and the voltage V_i applied via the gate capacitance C_g. Moreover, as shown in Fig. 1(a), the nearest-neighboring charge qubits in the three different link directions are coupled by different circuit elements:

(i) *X-type bond.* The two qubits [denoted by 1 and 2 in Fig. 1(a)] in the x-link direction are coupled by a mutual inductance M. This inductive coupling is given by [8] $K_x(1,2) = MI_1I_2$, where the circulating supercurrent I_i in the SQUID loop of the ith charge qubit is $I_i = I_c \sin(\pi\Phi_i/\Phi_0)\cos\varphi_i$, with $I_c = 2\pi E_J/\Phi_0$, $\Phi_0 = h/2e$ (the flux quantum) and φ_i being the average phase drop across the two Josephson junctions.

(ii) *Y-type bond.* The two qubits 1 and 3 in the y-link direction are coupled via an LC oscillator [9] and the inter-qubit coupling is $K_y(1,3) = -4\xi E_{J1}(\Phi_1)E_{J3}(\Phi_3)\sin\varphi_1\sin\varphi_3$, where $E_{Ji}(\Phi_i) = 2E_J\cos(\pi\Phi_i/\Phi_0)$, and $\xi = L[\pi C_\Sigma(C_g+C_m)/\Lambda\Phi_0]^2$, with

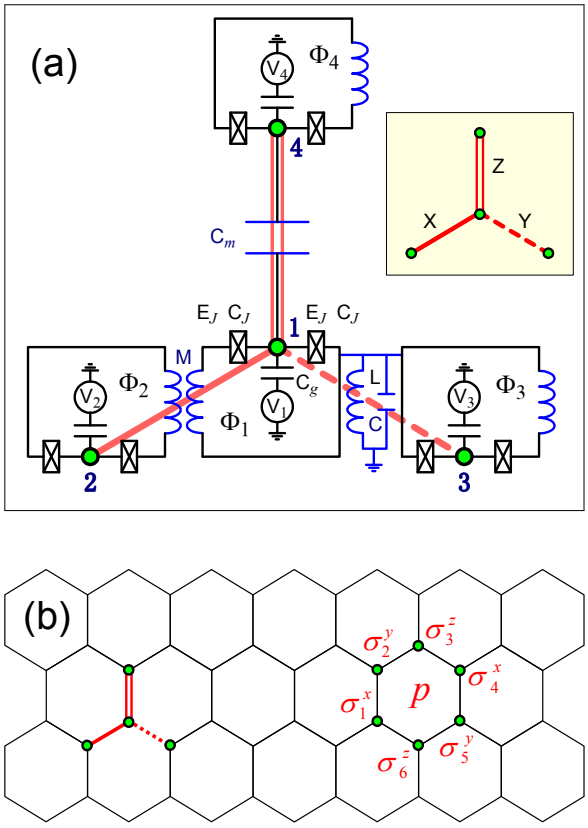

FIG. 1: (Color online) (a) Schematic diagram of the basic building block of a Kitaev lattice, consisting of four superconducting charge qubits (labelled 1 to 4): (i) The qubits 1 and 2 are inductively coupled via a mutual inductance M; (ii) the qubits 1 and 3 are coupled via an LC oscillator; and (iii) the qubits 1 and 4 are capacitively coupled via a mutual capacitance C_m. Inset: These three types of inter-qubit couplings are denoted as X, and Y and Z bonds. Here each charge qubit consists of a Cooper-pair box (green dot) which is linked to a superconducting ring, via two identical Josephson junctions (each with coupling energy E_J and capacitance C_J), to form a SQUID loop. Also, each qubit is controlled by both a voltage V_i (applied to the qubit via the gate capacitance C_g) and a magnetic flux Φ_i (piercing the SQUID loop). (b) A subset of the Kitaev lattice (honeycomb lattice) constructed by repeating the building block in (a), where a charge qubit is placed at each site. Also, the plaquette operator $W_p = \sigma_1^x\sigma_2^y\sigma_3^z\sigma_4^x\sigma_5^y\sigma_6^z$ is shown for a given plaquette (hexagon) p.

$C_\Sigma = 2C_J + C_g + C_m$, and $\Lambda = C_\Sigma^2 - C_m$. Note that $\xi \propto (C_g + C_m)^2$ in the presence of the mutual capacitance C_m that connects qubit 1 (3) with its nearest-neighboring qubit in the vertical (z-link) direction. Usually, $C_m \gg C_g$, so the coupling between qubits 1 and 3 is now much increased, compared to the usual case without the mutual inductance [9], where $\xi \propto C_g^2$.

(iii) *Z-type bond.* The two qubits 1 and 4 in the z-link direction are coupled via the mutual capacitance C_m [10, 11]: $K_z(1,4) = E_m(n_1 - n_{g1})(n_4 - n_{g4})$, where $E_m = 4e^2C_m/\Lambda$, $n_{gi} = C_gV_i/2e$, and $n_i = -i\partial/\partial\varphi_i$ is a number operator of the Cooper pairs in the ith box. The mutual capacitance C_m modifies the charging energy $2e^2/C_\Sigma$ of an isolated charge qubit to become $E_c = 2e^2C_\Sigma/\Lambda$.

When the electrostatic and the Josephson coupling energies of each charge qubit are included, the Hamiltonian of the lattice is $H = \sum_i[E_c(n_i - n_{gi})^2 - E_{Ji}(\Phi_i)\cos\varphi_i] + \sum_{\rm x-link} K_x(j,k) + \sum_{\rm y-link} K_y(j,k) + \sum_{\rm z-link} K_z(j,k)$. For charge qubits, $E_c \gg E_J$. When the gate voltage V_i is near the optimal point e/C_g, i.e., $n_{gi} \sim \frac{1}{2}$, only two charge states $|0\rangle_i$ and $|1\rangle_i$, corresponding to zero and one extra Cooper pairs in the box, are important for each qubit. In the spin-$\frac{1}{2}$ representation, based on the charge states $|0\rangle_i \equiv |\uparrow\rangle_i$ and $|1\rangle_i \equiv |\downarrow\rangle_i$, one has $n_i = \frac{1}{2}(1 - \sigma_i^z)$, $\cos\varphi_i = \frac{1}{2}\sigma_i^x$, and $\sin\varphi_i = -\frac{1}{2}\sigma_i^y$. Here we consider the simple case with $n_{gi} = n_g$ (i.e., $V_i = V_g$) and $\Phi_i = \Phi_e$ for all qubits. The Hamiltonian of the system is then reduced to

$$H = J_x \sum_{\rm x-link} \sigma_j^x\sigma_k^x + J_y \sum_{\rm y-link} \sigma_j^y\sigma_k^y + J_z \sum_{\rm z-link} \sigma_j^z\sigma_k^z + \sum_i (h_z\sigma_i^z + h_x\sigma_i^x). \quad (1)$$

This is the Kitaev model on a honeycomb lattice, in the presence of a "magnetic field" with z- and x-components. Here $h_z = (E_c + \frac{1}{2}E_m)(n_g - \frac{1}{2})$, and $h_x = -\frac{1}{2}E_J(\Phi_e)$, with $E_J(\Phi_e) = 2E_J\cos(\pi\Phi_e/\Phi_0)$. The bond parameters are $J_x = \frac{1}{4}MI_c^2\sin^2(\pi\Phi_e/\Phi_0) \geq 0$, $J_y = -\xi[E_J(\Phi_e)]^2 \leq 0$, and $J_z = \frac{1}{4}E_m > 0$. The magnetic field can be used to achieve single-qubit rotations for demonstrating anyonic braiding statistics.

Topological excitations.—Below we focus on two particular cases to show the properties of topological excitations in the Kitaev model (1):

(i) *Kitaev lattice in a weak magnetic field.* We first consider the case with $|h_z|, |h_x| \ll J_x, |J_y|, J_z$, and choose $V = \sum_i(h_z\sigma_i^z + h_x\sigma_i^x)$ as the perturbation. Using perturbation theory in the Green function formalism [3], one can construct an effective Hamiltonian $H_{\rm eff}$ acting on the vortex-free sector: $H_{\rm eff} = -(2h_z^2/\Delta\varepsilon_z)\sum_{\rm z-link}\sigma_j^z\sigma_k^z - (2h_x^2/\Delta\varepsilon_x)\sum_{\rm x-link}\sigma_j^x\sigma_k^x$, where $\varepsilon_{z(x)}$ is the excitation energy of the state $\sigma^{z(x)}|g\rangle$, and $|g\rangle$ is the eigenstate of all plaquette operators W_p [see Fig. 1(b)] corresponding to the eigenvalue $w_p = 1$. Here the effective Hamiltonian $H_{\rm eff}$ is only contributed by the second-order term because both the first- and third-order terms are zero. With the zeroth-order term (unperturbed Hamiltonian) included, the Hamiltonian of the system can be equivalently written as $H = J_x'\sum_{\rm x-link}\sigma_j^x\sigma_k^x + J_y\sum_{\rm y-link}\sigma_j^y\sigma_k^y + J_z'\sum_{\rm z-link}\sigma_j^z\sigma_k^z$, where the bond parameters J_z and J_x are renormalized to $J_z' = J_z - 2h_z^2/\Delta\varepsilon_z$, and $J_x' = J_x - 2h_x^2/\Delta\varepsilon_x$.

To show the topological excitations, we focus on the Abelian case [3] with $J_z' \gg J_x', |J_y|$. The dominant part of H, i.e., $H_0 = J_z'\sum_{\rm z-link}\sigma_j^z\sigma_k^z$, favors a highly degenerate

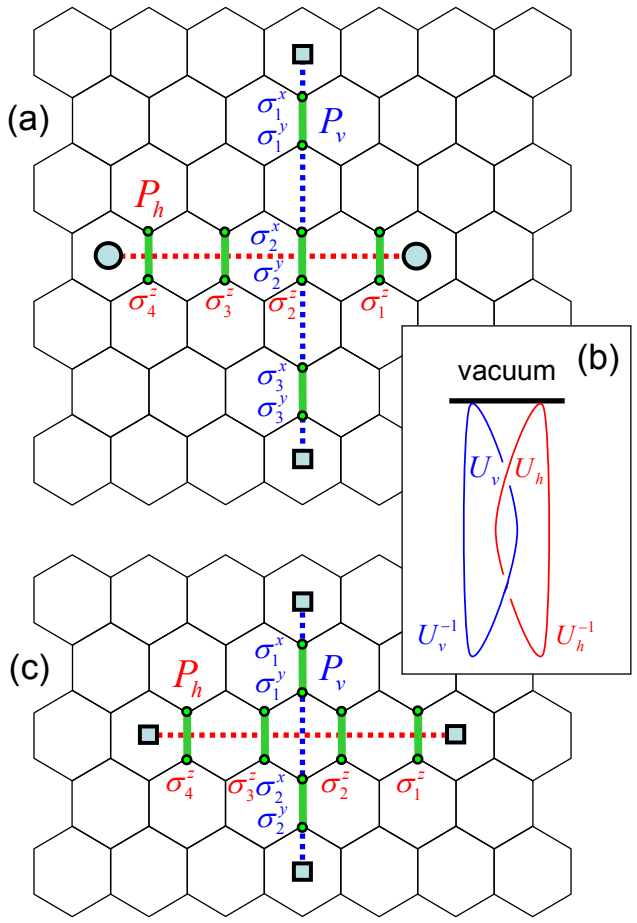

FIG. 2: (Color online) Schematic diagram of the procedures for braiding topological excitations. (a) The operations U_h and U_v for creating different types of topological excitations, which are achieved by successively applying spin-pair operators at z-bonds along the horizontal (P_h) and vertical (P_v) paths. (b) A combined operation $U_h^{-1}U_v^{-1}U_hU_v$ for both braiding the topological excitations created in (a) and fusing them to the vacuum. (c) The operations U_h and U_v for creating the same types of topological excitations, which are achieved by successively applying spin-pair operators at z-bonds along P_h and P_v.

ground state with each pair of spins in each z-link aligned opposite to each other ($|\uparrow\downarrow\rangle$ or $|\downarrow\uparrow\rangle$). While preserving the ground-state subspace, the effective Hamiltonian can now be written, up to fourth order, as

$$H_{\rm eff} = -J_{\rm eff}\sum_p W_p, \tag{2}$$

where $J_{\rm eff} = J_x'^2 J_y^2/16J_z'^3$. Clearly, the ground state of the system preserves $w_p = 1$, i.e., $W_p|g\rangle = |g\rangle$, for all plaquettes p. A pair of vortex excitations are created when the system changes with $w_p = 1 \to -1$ for two neighboring plaquettes. This can be achieved by acting a spin-pair operator on the ground state $|g\rangle$: $|\widetilde{Z}_i\rangle = \tilde{\sigma}_i^z|g\rangle$, and $|\widetilde{Y}_i\rangle = \tilde{\sigma}_i^y|g\rangle$, with $\tilde{\sigma}_i^z \equiv \sigma_i^z I_i$ and $\tilde{\sigma}_i^y \equiv \sigma_i^y\sigma_i^x$. Here the two operators σ_i^z (σ_i^y) and I_i (σ_i^x) act on the ground state $|g\rangle$ at the bottom and top sites of the ith z-link, respectively. This pair of vortex excitations are Abelian anyons [3, 6], which have an energy gap $\Delta\varepsilon = 4J_{\rm eff}$ above the ground state.

(ii) *Kitaev lattice with dominant z-bonds.* We choose $h_z = 0$, which corresponds to the case with each charge qubit working at the optimal point $n_g = \frac{1}{2}$. Moreover, we choose suitable circuit parameters to have $J_z \gg |h_x|, J_x, |J_y|$, with $|h_x|$ comparable to $J_x, |J_y|$. Here we also use perturbation theory in the Green function formalism to derive the effective Hamiltonian. Up to the second-order term, the effective Hamiltonian can be written as

$$H_{\rm eff} = -K_{\rm eff}\sum_{\rm z-link}\sigma_j^x\sigma_k^x, \tag{3}$$

with $K_{\rm eff} = h_x^2/J_z$. The spin-pair operator $\sigma_j^x\sigma_k^x$ at a z-bond is commutative with the unperturbed zero-order Hamiltonian $H_0 = J_z\sum_{\rm z-link}\sigma_j^z\sigma_k^z$, but anticommutative to the four plaquette operators W_p connected to this z-bond. Similar to W_p, the pair operator $\sigma_j^x\sigma_k^x$ also has two eigenvalues $p_z = \pm 1$. Now the ground state $|g\rangle$ of the system preserves $p_z = 1$, i.e., $\sigma_j^x\sigma_k^x|g\rangle = |g\rangle$, for all z-bonds. When the pair operators $\tilde{\sigma}_i^z$ and $\tilde{\sigma}_i^y$ are separately applied to the ground state at the ith z-bond, the excited states $|\widetilde{Z}_i\rangle = \tilde{\sigma}_i^z|g\rangle$, and $|\widetilde{Y}_i\rangle = \tilde{\sigma}_i^y|g\rangle$ are two types of bond states; each corresponding to the change $p_z = 1 \to -1$ at the ith z-bond and having an energy gap $2K_{\rm eff}$ above the ground state.

The braiding of topological excitations.—As shown in [6], an e-type vortex looping around another e vortex does not produce a sign change to the wave function, while an e vortex looping around an m-type vortex does. This indicates anyonic statistics between the e and m vortex states. Here we show an alternative procedure for braiding a topological excitation with another, which applies to both the vortex and bond states.

First, successively apply spin-pair operations $\tilde{\sigma}_i^y = \sigma_i^y\sigma_i^x$ to the ground state $|g\rangle$ at three z-bonds in the vertical path P_v [see Fig. 2(a)]. In the case of Hamiltonian (2), this creates a pair of e vortex states and move a vortex along the vertical path P_v, while a bond state is generated in the case of Hamiltonian (3). Then, we successively apply the operations $\tilde{\sigma}_i^z = \sigma_i^z I_i$ at four z-bonds along the horizontal path P_h [see also Fig. 2(a)]. After these operations, the state of the system is $U_hU_v|g\rangle$, where $U_h = \tilde{\sigma}_4^z\tilde{\sigma}_3^z\tilde{\sigma}_2^z\tilde{\sigma}_1^z$, and $U_v = \tilde{\sigma}_3^y\tilde{\sigma}_2^y\tilde{\sigma}_1^y$ correspond to the operations along the horizontal and vertical paths. Furthermore, successively apply U_v^{-1} and U_h^{-1} to the system, so as to fuse [1, 3] the excitations to the vacuum (i.e., the ground state) [see Fig. 2(b)]. Now, the final state of the system is $|\Psi_f\rangle = U_h^{-1}U_v^{-1}U_hU_v|g\rangle$. Because the paths P_v and P_h intersect at a lattice point, where $\tilde{\sigma}_2^y$ and $\tilde{\sigma}_2^z$ anticommute, one has $U_hU_v = -U_vU_h$. Therefore, the final

state becomes $|\Psi_f\rangle = -|g\rangle$. In contrast, for two topological excitations of the same type, when similar operations are applied, the paths P_v and P_h do not intersect at a lattice point [see Fig. 2(c)]. Thus, $U_h U_v = U_v U_h$, and $|\Psi_f\rangle = |g\rangle$, yielding no sign change to the ground-state wave function.

The braiding statistics of topological excitations can be revealed by means of Ramsey-type interference [6, 12]. To achieve this, we keep the same U_v as above, but use $U_h = (\tilde{\sigma}_4^z)^{\frac{1}{2}}(\tilde{\sigma}_3^z)^{\frac{1}{2}}(\tilde{\sigma}_2^z)^{\frac{1}{2}}(\tilde{\sigma}_1^z)^{\frac{1}{2}}$, where $(\tilde{\sigma}_i^z)^{\frac{1}{2}} \equiv (\sigma_i^z)^{\frac{1}{2}} I_i$, i.e., each σ_i^z is replaced by half of the rotation. In the braiding case shown in Fig. 2(a), $\tilde{\sigma}_2^y(\tilde{\sigma}_2^z)^{\frac{1}{2}} = i(\tilde{\sigma}_2^z)^{-\frac{1}{2}}\tilde{\sigma}_2^y$ at the crossing point of paths P_h and P_v. Thus, $|\Psi_f\rangle = U_h^{-1}U_v^{-1}U_h U_v|g\rangle = (\tilde{\sigma}_2^z)^{-\frac{1}{2}}[i(\tilde{\sigma}_2^z)^{-\frac{1}{2}}]|g\rangle = i|\widetilde{Z}_2\rangle$, similar to the case with an e vortex looping around a superposition state of an m vortex and the vacuum [6]. However, in the case without braiding [see Fig. 2(b)], $|\Psi_f\rangle = U_h^{-1}U_v^{-1}U_h U_v|g\rangle = |g\rangle$. Therefore, the braiding of topological excitations can be distinguished by verifying if an excited state $|\widetilde{Z}_2\rangle$ occurs at the crossing point of paths P_h and P_v.

Discussion and conclusion.—When the magnetic flux in the SQUID loop of each charge qubit is set to $\Phi_e = \Phi_0/2$, then $h_x = 0$ and $J_y = 0$. Also, we assume that $E_c \gg J_x, J_z$. When $\Phi_e = \Phi_0/2$, one can shift the gate voltage, at the ith lattice point, far away from the usual working point $n_g \sim \frac{1}{2}$ of the Kitaev lattice for a period of time τ. This yields a local z-type rotation on the ith qubit: $R_i^z(\theta) = \exp[-i(h_z\tau/\hbar)\sigma_i^z] \equiv \exp(-i\theta\sigma_i^z/2)$. When $\theta \equiv 2h_z\tau/\hbar = \pi$ (where $n_g > \frac{1}{2}$), $R_i^z(\pi) = -i\sigma_i^z$, so the σ_i^z operation on the ith qubit is given by $\sigma_i^z = e^{i\pi/2}R_i^z(\pi)$, while half of the rotation is $(\sigma_i^z)^{\frac{1}{2}} = e^{i\pi/4}R_i^z(\pi/2)$. The corresponding inverse rotations can be achieved by shifting the gate voltage to $n_g < \frac{1}{2}$. Similarly, when $n_g = \frac{1}{2}$ and $\Phi_e = 0$, one has $h_z = 0$, $h_x = -E_J$, and $J_x = 0$. Here we now assume that $E_J \gg |J_y|, J_z$. When $n_g = \frac{1}{2}$, we also switch off the flux in the SQUID loop of the ith qubit for a time τ (the working point of this Kitaev lattice is usually at $0 < \Phi_e < \Phi_0/2$). This produces a local x-type rotation on the ith qubit: $R_i^x(\theta) = \exp[i(\delta E_J\tau/\hbar)\sigma_i^x] \equiv \exp(i\theta\sigma_i^x/2)$, where $\delta E_J = E_J - \frac{1}{2}E_J(\Phi_e)$. The σ_i^x rotation on the ith qubit is $\sigma_i^x = e^{-i\pi/2}R_i^x(\pi)$, where $2\delta E_J\tau/\hbar = \pi$. With both σ_i^z and σ_i^x rotations available for the ith qubit, the σ_i^y rotation is given by $\sigma_i^y = e^{-i\pi/2}\sigma_i^z\sigma_i^x$. Therefore, one can construct the operations $\tilde{\sigma}_i^z$ and $\tilde{\sigma}_i^z$ for generating topological excitations by using the single-qubit rotations σ_i^z and σ_i^x.

In order to obtain accurate z- and x-type single-qubit rotations, we assume that E_c and E_J are much larger than the inter-qubit coupling. Actually, this strict condition can be loosened for realistic systems. As shown in [13], accurate effective single-qubit rotations can still be achieved using techniques from nuclear magnetic resonance when the inter-qubit coupling is small (instead of much smaller than E_c and E_J). In the vortex- and bond-state cases studied here, to reveal the braiding statistics of topological excitations, one should verify the occurrence of the excited state $|\widetilde{Z}_2\rangle$ at the crossing point of paths P_h and P_v. This needs to distinguish $|\widetilde{Z}_2\rangle$ from the ground state. Here the difference between $|\widetilde{Z}_2\rangle$ and the ground state is the phase flip, induced by the single-qubit rotation σ_i^z, on the charge state of the z-bond at the crossing point. This phase flip of the charge state could be measured, e.g., using state tomography [14].

In the region $J'_z \geq J'_x, |J_y|$, it is shown [15] that when acting on the ground state, the spin-pair operations $\tilde{\sigma}_i^z$ and $\tilde{\sigma}_i^y$ generally create both vortex states (Abelian anyons) and fermionic excitations. However, the weight of the anyons is dominant in the low-energy subspace if the number m of the spin-pair operations for braiding anyons is not large and $J'_z \gg J'_x, |J_y|$. Let $J'_x = |J_y| = J$. For example, when $m = 25$, $\gamma \equiv J/J'_z$ can be $\gamma \sim 0.2$ [15].

In conclusion, we have proposed an approach to realize the Kitaev model on a honeycomb lattice using superconducting quantum circuits. Two particular cases are studied to demonstrate the topological states and the braiding statistics. Our approach provides an experimentally realizable many-body system for demonstrating exotic properties of these topological phases.

F.N. was supported in part by the NSA, LPS, ARO, and the NSF Grant No. EIA-0130383. J.Q.Y. and X.F.S. were supported by the "973" Program Grant Nos. 2009CB929300 and 2006CB921205, and the NSFC Grant Nos. 10625416 and 10534060.

[1] C. Nayak, S.H. Simon, A. Stern, M. Freedman, and S. Das Sarma, arXiv: 0707.1889 (to be published in Rev. Mod. Phys.), and references therein.
[2] S. Das Sarma, M. Freedman, and C. Nayak, Phys. Rev. Lett. **94**, 166802 (2005).
[3] A. Kitaev, Ann. Phys. (N.Y.) **321**, 2 (2006).
[4] L.-M. Duan, E. Demler, and M.D. Lukin, Phys. Rev. Lett. **91**, 090402 (2003).
[5] A. Micheli, G.K. Brennen, and P. Zoller, Nature Phys. **2**, 341 (2006).
[6] C. Zhang, V.W. Scarola, S. Tewari, and S. Das Sarma, Proc. Natl. Acad. Sci. U.S.A. **104**, 18415 (2007).
[7] See, e.g., J.Q. You and F. Nori, Phys. Today **58**, No. 11, 42 (2005).
[8] J.Q. You, J.S. Tsai, and F. Nori, Phys. Rev. Lett. **89**, 197902 (2002).
[9] Y. Makhlin, G. Schön, and A. Shnirman, Nature **398**, 305 (1999).
[10] Yu. A. Pashkin *et al.*, Nature (London) **421**, 823 (2003).
[11] F. Marquardt and C. Bruder, Phys. Rev. B **63**, 054514 (2001).
[12] J.K. Pachos, Ann. Phys. (N.Y.) **322**, 1254 (2007).
[13] L.F. Wei, Y.X. Liu, and F. Nori, Phys. Rev. B **72**, 104516 (2005).

[14] Y.X. Liu, L.F. Wei, and F. Nori, Phys. Rev. B **72**, 014547 (2005); M. Steffen *et al.*, Science **313**, 1423 (2006).
[15] S. Dusuel, K.P. Schmidt, and J. Vidal, Phys. Rev. Lett. **100**, 177204 (2008).